A&A 408, 729–736 (2003)
DOI: 10.1051/0004-6361:20031014

Astronomy & Astrophysics

Study of *p*-mode excitation and damping rate variations from IRIS^{++} observations

D. Salabert[1,2], S. J. Jiménez-Reyes[3], and S. Tomczyk[4]

[1] Laboratoire Universitaire d'Astrophysique de Nice, Université de Nice-Sophia Antipolis, 06108 Nice Cedex 2, France
[2] School of Physics and Astronomy, University of Birmingham, Edgbaston, Birmingham B15 2TT, UK
[3] Themis, Instituto de Astrofísica de Canarias, 38701, La Laguna, Tenerife, Spain
[4] High Altitude Observatory, NCAR, PO Box 3000, Boulder, CO 80307, USA

Received 31 March 2003 / Accepted 4 June 2003

Abstract. 11 years of low degree helioseismic data collected by the IRIS^{++} network (*International Research of the Interior of the Sun*) have been analyzed. The epoch covered (mid-1989 to end-1999) spans the maximum and the falling phase of solar cycle 22 and the rising phase of the current solar cycle 23. Annual timeseries with an overlap of 6 months are used to study the variations with solar activity of the *p*-mode frequencies $\nu_{n,\ell}$, heights $H_{n,\ell}$, and linewidths $\Gamma_{n,\ell}$, taking into account the effects of the window function. These are used to infer variations in the velocity power $< V^2_{n,\ell} >$ and the energy supply rate $\dot{E}_{n,\ell}$ which relate to changes in the excitation and the damping of the modes. We find global changes over the range $2600 \leq \nu \leq 3600$ μHz of about -26%, 11%, -11% for the heights, the linewidths, and the velocity power respectively, and a constant energy supply to the modes.

Key words. Sun: helioseismology – Sun: activity

1. Introduction

Acoustic mode parameters have been demonstrated to be very sensitive to the solar activity cycle. The first report given by Woodard & Noyes (1985) uncovered a frequency shift for low degrees of around 0.4 μHz. This result was soon confirmed by Fossat et al. (1987) for low degrees. Libbrecht & Woodard (1990) shown using measurements of intermediate-ℓ ($5 \leq \ell \leq 100$) that these frequency shifts are greater with higher degrees. Magnetic field changes are believed to be the most likely source of these shifts (Goldreich et al. 1991; Dziembowski et al. 2001), either directly – via the action of the Lorentz force – or indirectly by changing the entropy stratification in the solar cavity. Some evidence was obtained that modes with different degrees ℓ and azimuthal orders m have different sensitivities to magnetic flux, depending on the positions of the activity on the solar surface (Jiménez-Reyes et al. 1998; Salabert et al. 2002a). Correlations of a few months between frequency shifts and solar activity indexes were observed in low-ℓ by Chaplin et al. (2001) and Salabert et al. (2002c).

Afterwards, new aspects of the mode parameter variations were revealed. Using 12 years of Mark-I data from 1977 to 1989, Pallé et al. (1990a,b) have reported an increase of about 30% for the linewidths with increasing activity and a variation between 30 and 40% in the power anticorrelated with solar activity, which was confirmed later by Anguera Gubau et al. (1992) explaining that a variation of about 15% of the characteristic size of the solar granules between maximum and minimum of solar activity would account for the observed effect. However, accurate estimations of these parameters require long and well-filled datasets of high quality, thus the analyses following Pallé's ones using generally single site observations sometimes present contradictory results, especially for the linewidth observations (Meunier 1997). The deployment of helioseismic ground-based networks (like IRIS, BiSON or GONG) and their running over several years has improved the accuracy of the estimations: the recent claims from Chaplin et al. (2000) and Komm et al. (2000a) about the changes of these parameters, showing very good agreement, are therefore much more certain.

In the low-ℓ data from the BiSON network, Chaplin et al. (2000) have observed a mean increase of $24 \pm 3\%$ in the linewidths from 1991 to 1997 over the frequency range $2600 \leq \nu \leq 3600$ μHz; a decrease of $22 \pm 3\%$ in the velocity power and on average, no variation for the energy rate supplied to the modes. However during a brief period of a few months in the beginning of 1998, Chaplin et al. (2003) showed that the energy supply rate for the low degrees increased significantly, when major surface activity of the Sun was occuring, as indicated by flares, CMEs and particle fluxes.

The analysis of the intermediate degrees ($\ell \leq 150$) from the GONG network shows an increase of about 10% for the

Send offprint requests to: D. Salabert,
e-mail: david.salabert@unice.fr

mode widths from 1995 to 1998 in the frequency range 2.7 and 3.3 mHz with increasing activity (Komm et al. 2000a). At the same time, the mode height decreases 21% while the mode area (width × height) decreases by 18%. The analysis found no ℓ dependence in the solar cycle changes, however the values of the variations change with smaller-ℓ values. As a function of frequency, these changes show a maximum between 2.7 and 3.3 mHz. Komm et al. (2000b) have observed that the energy supply rate $\dot{E}$ decreases with increasing activity, showing the largest decrease of $-4.4 \pm 4.3\%$ in the range $15 \leq \ell \leq 95$ and $1.6 \leq \nu \leq 3.1$ mHz, with almost no frequency or ℓ dependence. For $\nu > 3.1$ mHz and $\ell \geq 15$, the average value is close to zero, showing no frequency dependence, which is in sharp contrast to the other parameters. Recently, Komm et al. (2002) have reported a global decrease between mid-1995 and mid-2001 of $\dot{E}$ of about -6%.

While unambiguous changes to the mode height and width have now been identified, the current challenge is to study these in greater detail (i.e. with better accuracy and precision). In the present work, we make use of the IRIS^{++} database which has collected solar observations for almost a complete solar cycle to study the signature of solar activity for the *p*-mode parameters, focusing our attention on variations of the excitation and damping parameters. By means of these results, we analyze the variation of the velocity power of the low degree modes and the energy supplied to them.

2. Data analysis

The IRIS^{++} network (*International Research of the Interior of the Sun*) is composed of the original IRIS sodium instruments which have been merged with the Mark-I potassium resonant scattering spectrophotometer (Brookes et al. 1978) (which is part of the BiSON network) located at the Observatorio del Teide (Tenerife, Spain), and the Magneto-Optical Filter LOWL potassium instrument (Tomczyk et al. 1995) located in Mauna Loa (Hawaii, USA). The merging of these different observations in a consistent manner (Salabert et al. 2002b) to give them similar sensitivity results in an important improvement in the network duty cycle thanks to the wide distribution of the instrument longitudes. The merged observations consist of a timeseries of measurements of the solar line-of-sight velocity integrated over the solar surface. The full-disk integration gives access to low degree modes, with $\ell \leq 3$. The observations covering 11 years from July 1st 1989 to November 05 1999, span the maximum and the falling phase of solar cycle 22 and the rising phase of the current solar cycle 23. They were divided into 20 timeseries of 360 days with an overlap of 180 days. The duty cycle of the timeseries before LOWL is included in the database in 1994 (LOWL operation started in February 1994) is about 40% whereas it is more than 60% after 1994 when LOWL data are included. Figure 1 shows that the duty cycle is "anti-correlated" with the solar activity. This means that we have to be very careful in the analysis of the *p*-mode parameter changes over the solar activity cycle, especially for the heights and the linewidths (and the combinations of them), which are very dependent on the duty cycle and the presence of the sidelobes. Then, before any analyses are made for changes with solar activity, the influence of each window function on each parameter needs to be studied.

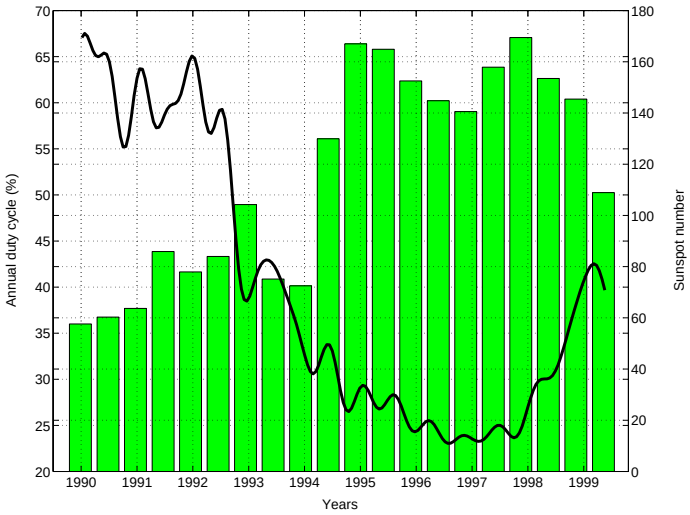

Fig. 1. Duty cycle of the 20 timeseries analyzed, compared to a solar activity index (solid line), here the R_I International Sunspot Number.

3. Modeling the acoustic mode spectrum

It is generally accepted that the acoustic modes are stochastically excited and intrinsically damped by convection and turbulent viscosity (Kumar et al. 1988). Therefore, the analogy for the *p*-modes is a forced and damped oscillator:

$$\frac{\mathrm{d}^2 q(t)}{\mathrm{d}t^2} + 2\eta \frac{\mathrm{d}q(t)}{\mathrm{d}t} + 4\pi\nu_0^2 q(t) = f(t) \tag{1}$$

where t is the time, $q(t)$ the displacement, η the damping constant, ν_0 the temporal frequency of the undamped oscillator, and $f(t)$ the random forcing function. The average power spectrum of the oscillator equation $\mathcal{P}_q(\nu) = < |\tilde{q}(\nu)|^2 >$ in the vicinity of resonance ($\nu \sim \nu_0$) with $\eta \ll \nu_0$ may be written as:

$$\mathcal{P}_q(\nu) = \frac{\mathcal{P}_f(\nu)}{4\pi^2(\nu^2 - \nu_0^2)^2 + \eta^2} \simeq \frac{1}{16\pi^2\nu_0^2} \frac{\mathcal{P}_f(\nu)}{(\nu - \nu_0)^2 + \eta^2} \tag{2}$$

where $\mathcal{P}_f(\nu) = < |\tilde{f}(\nu)|^2 >$ is the power spectrum of the forcing function $f(t)$, which varies slowly with ν_0. $\tilde{q}(\nu)$ and $\tilde{f}(\nu)$ are the Fourier transforms of $q(t)$ and $f(t)$. $\mathcal{P}_q(\nu)$ is a very good approximation of a Lorentzian profile. For a given mode (n, ℓ) with a temporal frequency $\nu_{n,\ell}$, the full-width at half-maximum $\Gamma_{n,\ell}$ of the profile is related to the damping rate $\eta_{n,\ell}$ by:

$$\Gamma_{n,\ell} = \frac{\eta_{n,\ell}}{\pi}. \tag{3}$$

The peak height $H_{n,\ell}$ is given by:

$$H_{n,\ell} = \frac{\mathcal{P}_{f_{n,\ell}}(\nu)}{16\pi^2\nu_{n,\ell}^2\eta_{n,\ell}^2} = \frac{\mathcal{P}_{f_{n,\ell}}(\nu)}{16\pi^3\nu_{n,\ell}^2\Gamma_{n,\ell}^2}. \tag{4}$$

The total velocity power $< V^2_{n,\ell} >$ is proportional to the height $H_{n,\ell}$ times the linewidth $\Gamma_{n,\ell}$, which corresponds to the area under the mode:

$$< V^2_{n,\ell} > = \frac{\pi}{2} C_{\rm obs} H_{n,\ell} \Gamma_{n,\ell} = \frac{C_{\rm obs}}{32\pi^3} \frac{\mathcal{P}_{f_{n,\ell}}(\nu)}{\nu^2_{n,\ell} \Gamma_{n,\ell}} \quad (5)$$

where the factor $(\pi/2)$ is a scaling factor for the area under a Lorentz profile and $C_{\rm obs}$ is a constant to correct for the effects of the observation techniques.

The total energy in the modes $E_{n,\ell}$ can be written as the sum of kinetic and potential energy:

$$E_{n,\ell} = \mathcal{M}_{n,\ell} < V^2_{n,\ell} > \quad (6)$$

where $\mathcal{M}_{n,\ell}$ is the corresponding mode mass which is defined as the product of mode inertia $I_{n,\ell}$, multiplied by the solar mass $\mathcal{M}_\odot$:

$$\mathcal{M}_{n,\ell} = 4\pi \mathcal{M}_\odot I_{n,\ell} \quad (7)$$

where 4π is a factor of normalization, and the mode inertia $I_{n,\ell}$ is written as:

$$I_{n,\ell} = \frac{1}{\mathcal{M}_\odot |\delta r_{\rm phot}|^2} \int_V \rho |\delta r|^2 {\rm d}V \quad (8)$$

where ρ is the density, δr is the displacement associated with the oscillation, $\delta r_{\rm phot}$ is the displacement at the photospheric radius, and integration is over the volume V of the Sun (Christensen-Dalsgaard & Berthomieu 1991). $\mathcal{M}_{n,\ell}$ is assumed to be constant over all the timeseries analyzed for each (n, ℓ), thus variations of energy and velocity power are equal.

The rate at which the energy is supplied to the modes $\dot{E}_{n,\ell}$ is estimated by (Goldreich et al. 1994):

$$\frac{{\rm d}E_{n,\ell}}{{\rm d}t} = \dot{E}_{n,\ell} = 2\pi E_{n,\ell} \Gamma_{n,\ell} = \frac{C_{\rm obs} \mathcal{M}_{n,\ell}}{16\pi^2} \frac{\mathcal{P}_{f_{n,\ell}}(\nu)}{\nu^2_{n,\ell}}. \quad (9)$$

Looking for temporal variations, the fractionnal changes of these parameters can be written:

$$\frac{\delta \Gamma_{n,\ell}}{\Gamma_{n,\ell}} = \frac{\delta \eta_{n,\ell}}{\eta_{n,\ell}} \quad (10)$$

$$\frac{\delta H_{n,\ell}}{H_{n,\ell}} = \frac{\delta \mathcal{P}_{f_{n,\ell}}}{\mathcal{P}_{f_{n,\ell}}} - 2\frac{\delta \eta_{n,\ell}}{\eta_{n,\ell}} \quad (11)$$

$$\frac{\delta < V^2_{n,\ell} >}{< V^2_{n,\ell} >} = \frac{\delta \mathcal{P}_{f_{n,\ell}}}{\mathcal{P}_{f_{n,\ell}}} - \frac{\delta \eta_{n,\ell}}{\eta_{n,\ell}} \quad (12)$$

$$\frac{\delta \dot{E}_{n,\ell}}{\dot{E}_{n,\ell}} = \frac{\delta \mathcal{P}_{f_{n,\ell}}}{\mathcal{P}_{f_{n,\ell}}}. \quad (13)$$

These parameters provide information about different phenomena. Thus, the linewidth $\Gamma_{n,\ell}$ is a direct measure of the damping rate, meaning that any changes in $\Gamma_{n,\ell}$ with solar activity implies a change in the damping rate $\eta_{n,\ell}$ (Eq. (10)). The velocity power $< V^2_{n,\ell} >$ represents the equilibrium between the excitation $\mathcal{P}_{f_{n,\ell}}$ and the damping $\eta_{n,\ell}$ of the modes (Eq. (12)). Change in the energy supply rate $\dot{E}_{n,\ell}$ with solar activity implies a variation in the net forcing $\mathcal{P}_{f_{n,\ell}}$ (Eq. (13)).

3.1. Line fitting

The *p*-mode parameters have been extracted by fitting a Lorentzian profile (Eq. (2)) with an additive background noise *B*, constant in the fitted frequency interval. The observed asymmetries on *p*-mode profiles (Duvall et al. 1993; Toutain et al. 1998; Chaplin et al. 1999a; Chaplin & Appourchaux 1999b; Thiery et al. 2000; Gelly et al. 2002) are explained to be caused by the interaction between the waves and a part of the background noise (Nigam & Kosovichev 1998). However, the observations to date have failed to uncover significant evidence for any variation of this parameter with solar activity (Appourchaux 2001; Gelly et al. 2002). Looking for fractional changes in the *p*-mode parameters, we assume that each *m*-component is well represented by a symmetric Lorenztian profile. The first temporal sidelobes were included in the model and the study of each temporal window function determines the ratio between the height of the main peak and the height of the corresponding sidebands (see Sect. 3.2). The pairs of even degree ($\ell = 0, 2$) and odd degree modes ($\ell = 1, 3$) were fitted together because the presence of the 11.57 μHz sidebands which complicate the structure of the power spectrum. The rotational splitting is taken to be constant and equal to 400 nHz. We constrained the linewidth to be the same for all the components of the two multiplets. The relative *m*-components height ratio $H_{n,\ell,m}/H_{n,\ell}$ are constrained to take the theoretical value for an instrument without spatial resolution for the case of observations using the sodium line (Christensen-Dalsgaard 1989). The *p*-mode parameters are then extracted using the Powell minimization algorithm (Press et al. 1992), by means of a standard maximum likelihood function with a χ^2 distribution. The mode parameters were varied progressively or in different steps until they converged to their best fit. The natural logarithm of the heights, the linewidths, and the background noise have been fitted, not the parameters themselves, resulting in a normal distribution which allows the uncertainties on each parameter to be determined from the inverse Hessian matrix.

Some bias on the mode widths and the mode heights arise from a combination of the effects of the window function and of the inherent quality of the data set. The extracted width will be overestimated by the fitting procedure and the extracted height will be underestimated, because of the width-height anticorrelation. We need to correct the returned fitted values for the window function effects before any analysis, which will be developed in terms of the logarithmic values. Then variations obtained in $\log(H_{n,\ell})$ and $\log(\Gamma_{n,\ell})$ or the additive combinations of the two correspond to fractional variations in $H_{n,\ell}$ and in $\Gamma_{n,\ell}$ and the multiplicative combinations of the two.

3.2. Window function correction

The effect of a window function that contains both diurnal and random breaks (due to the day/night cycle and bad weather and occasional instrument breakdown), and thus a duty cycle less than 100 per cent, is to redistribute power from the main lobe into the sidelobes and into the background. Therefore, the height and linewidth of a peak in the power spectrum depends on the characteristics of the temporal window, especially the

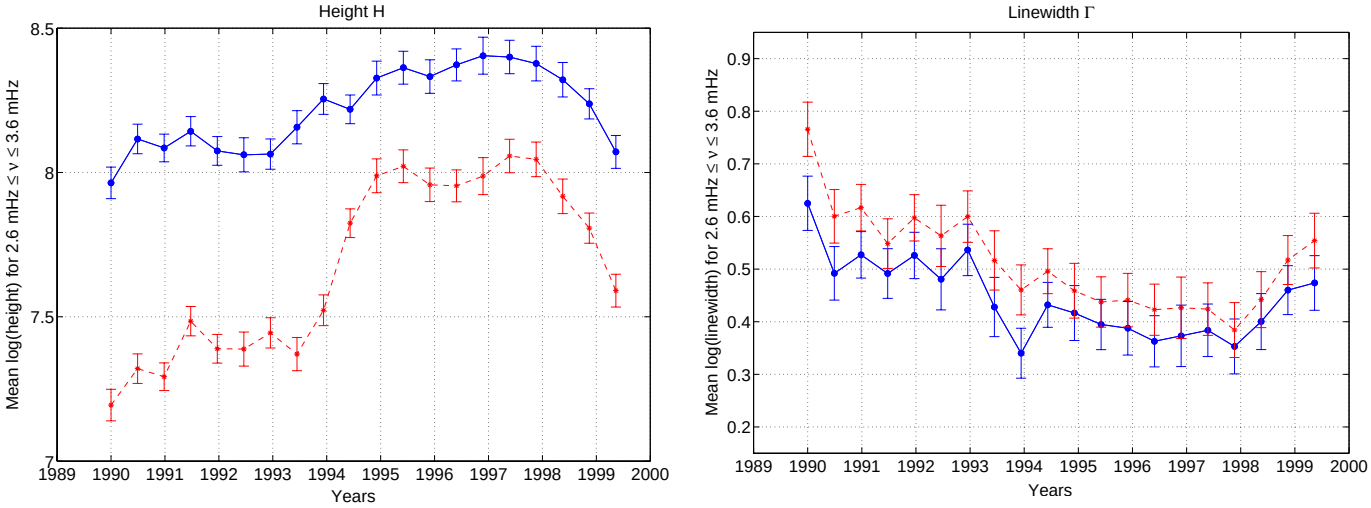

Fig. 2. The mean height (left part) and the mean linewidth (right part) in the frequency range 2.6 mHz $\leq \nu \leq$ 3.6 mHz for $\ell = 0, 1, 2, 3$ (in natural logarithmic units) before (dashed line) and after (solid line) correction.

duty cycle. The best way to remove its effects is to convolve the fit model with the window function. This process is computationally intensive and was not used. Instead, we simulated the effect of the temporal window as follows: we computed a window function for the timeseries and normalized it to unity; this was convolved with a Lorentzian with unit height and full-width of 1 μHz, which is a typical value for the range of modes studied in this analysis (moreover, the results are not very sensitive to the value chosen). This simulated spectrum was then fit by least-squares to yield the peak height, the sidelobe height, and the width of the Lorentzian. The factors are computed by taking the true linewidth (or the true height) and dividing by the fitted linewidth (or the fitted height) respectively. The corrections are made by multiplying the results obtained from the iterative fits by these corrective factors. The mean correcting factors $\overline{\alpha}_x$ (x being the height H or the linewidth Γ) before LOWL is included in the database are $\overline{\alpha}_H \sim 2.07$ and $\overline{\alpha}_\Gamma \sim 0.91$, whereas the mean correcting factors $\overline{\beta}_x$ after the inclusion of LOWL data are $\overline{\beta}_H \sim 1.48$ and $\overline{\beta}_\Gamma \sim 0.95$. These values confirm that the fitting procedure overestimates the linewidths and underestimates the heights, the effect of the window function being larger on the heights than on the linewidths. Both mode parameters depend strongly on the duty cycle and also on the complex way in which the gaps are distributed in the timeseries from multisite observations. However, we do not find a clear frequency dependence, in contradiction to what Komm et al. (2000a) have found with intermediate degree GONG data. Figure 2 shows the mean height (left part) and the mean linewidth (right part) between the frequencies 2.6 mHz and 3.6 mHz for $\ell = 0, 1, 2, 3$ (in natural logarithmic units) before (dashed line) and after (solid line) correction. The heights are largely underestimated, the mismatch being larger with low duty cycle. The merging of LOWL data in February 1994 clearly improves the estimations, but corrections are still needed.

The simulation is performed for a singlet peak only, whereas multi-component doublets are fitted (by necessity, owing to their proximity in frequency) in the real data. As such, the interaction of several closely-spaced components with the window function may be rather more complicated than is the case for a single, isolated component only. The interaction with, and effects of, the window may be slightly different in the real data and this point will be studied in a future work.

4. Solar activity variation

4.1. Time variation

Once the heights and the linewidths are corrected for the window function effects, we have computed the mean values of each parameter ($\nu_{n,\ell}$, $\log(H_{n,\ell})$, $\log(\Gamma_{n,\ell})$, $\log(< V^2_{n,\ell} >)$, $\log(\dot{E}_{n,\ell})$) for each degree $\ell = 0, 1, 2, 3$ in the frequency range $2600 \leq \nu \leq 3600$ μHz. The difference is computed with a reference taken as the average of 6 consecutive power spectra during the minimum of solar activity from 05 June 1994 to 15 November 1997, weighted by the uncertainties. Thus we obtain the fractional changes in percent along the 11 years analyzed.

The global changes over the 20 timeseries analyzed for each of these parameters are also determined. We compute a weighted linear fit between each parameter and the corresponding mean values of the 10.7 cm radio flux (in RF units), which is a proxy for the level of the solar activity, observed over the duration of each timeseries used (note that 1 RF unit corresponds to 10^{-22} W m^{-2} Hz^{-1}). For example, we can write for the frequency shift $\Delta\nu_{n,\ell}$:

$$\Delta\nu_{n,\ell} = a + b \times RF \tag{14}$$

$$\Delta\nu_{n,\ell}(\max) - \Delta\nu_{n,\ell}(\min) = b \times [RF(\max) - RF(\min)] \tag{15}$$

where b and a are the resulting slope and intercept of the linear fit respectively. $RF(\max) = 190.57 \times 10^{-22}$ W m^{-2} Hz^{-1} is the radio flux during the maximum of activity, taken as the mean value between 1989 July 01 and 1992 June 14. $RF(\min) = 75.86 \times 10^{-22}$ W m^{-2} Hz^{-1} is the corresponding average radio flux during the minimum of activity from 1994 June 05 to 1997 November 15.

Table 1. Global changes averaged over the frequency range $2600 \leq \nu \leq 3600$ μHz for the degrees $0 \leq \ell \leq 3$. The Spearman correlation coefficient r_s and the associated probability of having no correlation P_s between variations of each parameter and the 10.7 cm radio flux, used as a proxy of the solar cycle, are also shown. These values were computed with the extracted *p*-mode parameters from 10 independent timeseries of 360 days.

Parameters	Global changes	r_s	P_s
Frequency $\nu_{n,\ell}$	0.28 ± 0.02 μHz	+0.89	5.42e−04
Height $H_{n,\ell}$	-25.81 ± 1.94%	−0.85	1.58e−03
Linewidth $\Gamma_{n,\ell}$	11.19 ± 0.72%	+0.94	5.48e−05
Velocity power $< V^2_{n,\ell} >$	-11.40 ± 1.39%	−0.81	3.44e−03
Energy supply rate $\dot{E}_{n,\ell}$	0.48 ± 1.54%	−0.40	0.15

Equation (15) gives the global change for the frequency $\nu_{n,\ell}$ over the 11 years analyzed. The same kind of computation is done for $H_{n,\ell}$, $\Gamma_{n,\ell}$, $< V^2_{n,\ell} >$ and $\dot{E}_{n,\ell}$ (Table 1). We have also evaluated the degree of correlation between the variations of each parameter and the 10.7 cm radio flux. Table 1 shows the Spearman correlation coefficient r_s and its two-sided significance P_s, i.e. the probability of having null correlation. The results shown in Table 1 are obtained using the extracted parameters from 10 independent timeseries of 360 days.

Figure 3 shows the well-known frequency shift changes $\Delta\nu_{n,\ell}$ over the solar activity cycle. The solid line corresponds to the mean value of degrees $\ell = 0, 1, 2, 3$ between 2.6 and 3.6 mHz, weighted by the uncertainties. A global change of $\Delta\nu_{n,\ell=0,1,2,3} = 0.28 \pm 0.02$ μHz between the maximum and the minimum of solar activity is found, which is slightly smaller than the previous cycle. The activity indexes also show that the maximum of cycle 23 is smaller than the maximum of cycle 22 (Ahluwalia 2002). For example, the average sunspot number during the maximum of cycle 22 is about 150, whereas during the last maximum the mean sunspot number is about 110. The development of cycle 23 is different from cycle 22, especially the unusually short time cycle 22 took to reach its maximum. The current solar cycle compares better to cycles 17 and 20 (more information can be found at `http://www.dxlc.com/solar/`).

The upper panels of Fig. 4 show the variations of the heights $H_{n,\ell}$ and the linewidths $\Gamma_{n,\ell}$. The evolution with solar activity is quite clear, the heights $H_{n,\ell}$ being anti-correlated and the linewidths $\Gamma_{n,\ell}$ being correlated with the solar activity cycle, which is shown well by the correlation coefficients (see Table 1). We found a global change of -25.81 ± 1.94% for the heights and 11.19 ± 0.72% for the linewidths. Regarding the velocity power $< V^2_{n,\ell} >$ (lower panels of Fig. 4), it is well anti-correlated with the solar activity, showing a variation of -11.40 ± 1.39%. For the energy supply rate $\dot{E}_{n,\ell}$, in which a change of 0.48 ± 1.54% is found, we can consider that no variation is observed and it remains constant with solar activity. The associated probability of having no correlation is not significant and is consistent with zero change. We do not observe the increase in the energy supply rate as presented by Chaplin et al. (2003) during the first months of 1998. To confirm this, analyses with shorter timeseries are needed.

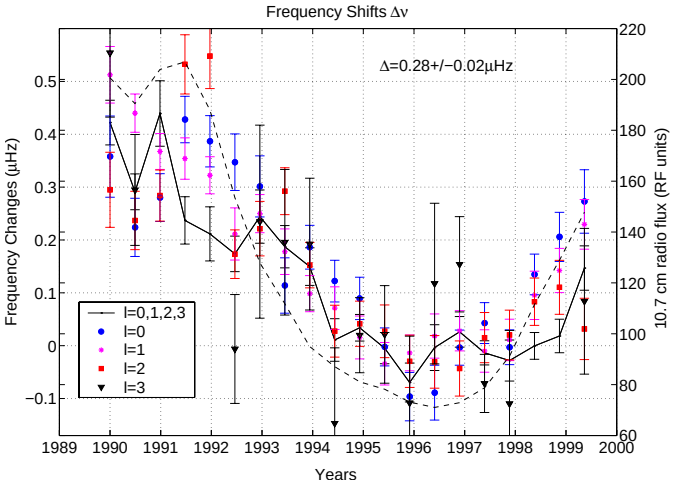

Fig. 3. Relative mode frequency differences $\nu_{n,\ell}$ versus time. For comparison, the variation of the 10.7 cm radio flux is plotted as a dashed line. (Note that in this figure, the plotted points for each mode are not independent, whereas the global change coefficients in Table 1 were computed from independent points.)

Our results are in good agreement with the recent ones of Jiménez-Reyes et al. (2001) with Mark-I data from 1984 to 1999. These authors have observed a decrease of about 20% in the total velocity power, defined as the energy below the *p*-mode profiles between the minimum and the maximum of solar cycle 22, using a cross-correlation technique. They have also separated the contributions of the velocity power for the even ($\ell = 0, 2$) and odd ($\ell = 1, 3$) modes, which are better correlated around the maximum than the minimum. Moreover, the changes uncovered for even and odd modes have similar heights. They have reported a "bump" in the middle of the maximum of activity close to 1990. In Fig. 4c, we can also observe a "bump" centered on the maximum of activity around mid-1990.

4.2. Frequency dependence

We now study the frequency dependence of the *p*-mode parameters variations. To do so, a weighted linear fit is computed at each (n, ℓ) between each parameter and the corresponding values of the mean 10.7 cm radio flux (in RF units), as was done in the previous subsection using Eq. (14). The gradient of the fit represents the global change of the parameter per unit of the radio flux used here again as a proxy of the solar cycle.

In Fig. 5 the frequency shifts $\Delta\nu_{n,\ell}$ versus frequency can be seen. It shows an important increase with frequency between 2.5 mHz and 3.6 mHz; below 2.5 mHz, the frequency shifts are small but positive. A change of about 4 nHz/RF at 3.6 mHz is observed. The solid line corresponds to the mean value of degrees $\ell = 0, 1, 2, 3$ for each order *n*, weighted by the uncertainties.

The upper panels of Fig. 6 show the changes obtained for the heights $H_{n,\ell}$ and the linewidths $\Gamma_{n,\ell}$ respectively over the frequency range from 1.9 mHz to 3.6 mHz. The height changes are clearly negative, meaning a decrease of the heights with an increase of solar activity. As for the linewidths $\Gamma_{n,\ell}$, their changes are clearly positive, implying an increase in the damping rate $\eta_{n,\ell}$. The lower panels of Fig. 6 illustrate the changes

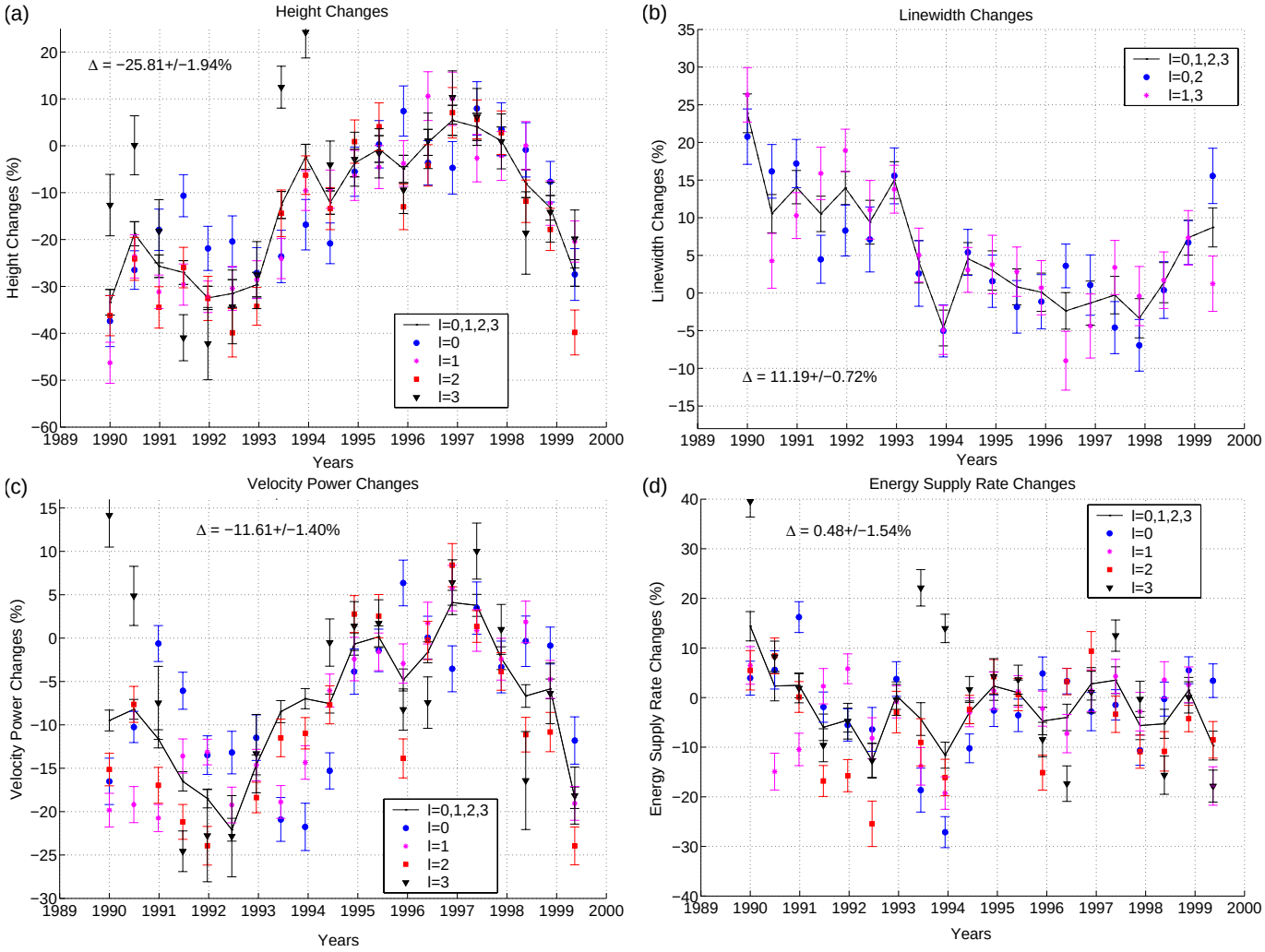

Fig. 4. Relative differences versus time for **a)** the height $H_{n,\ell}$, **b)** the linewidth $\Gamma_{n,\ell}$, **c)** the velocity power $< V^2_{n,\ell} >$ and **d)** the energy supply rate $\dot{E}_{n,\ell}$. (Note that in these figures, the plotted points for each mode are not independent, whereas the global change coefficients in Table 1 were computed from independent points.)

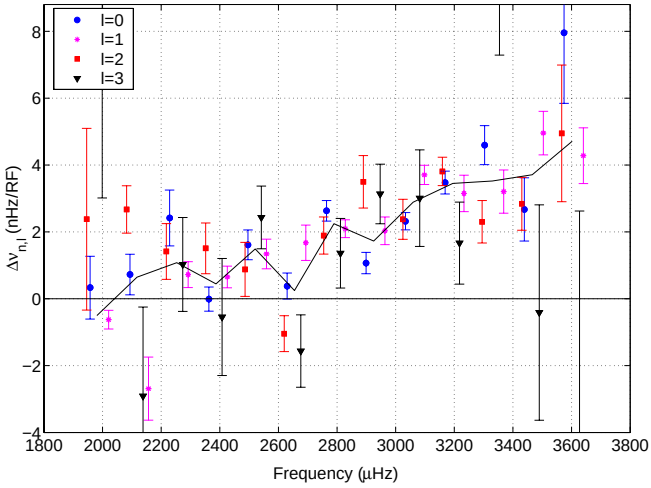

Fig. 5. Relative mode frequency differences $\nu_{n,\ell}$ per unit of radio flux (RF) versus frequency.

in the velocity power $< V^2_{n,\ell} >$ and in the energy supply rate $\dot{E}_{n,\ell}$ respectively. The velocity power $< V^2_{n,\ell} >$ decreases with increasing activity, whereas no variation is observed in the energy supply rate $\dot{E}_{n,\ell}$, meaning that the net forcing function $\mathcal{P}_{f_{n,\ell}}$ remains constant with solar activity.

The changes of the *p*-mode parameters with solar activity obtained in this analysis are very similar to those observed by Jiménez et al. (2002) using data from the space experiment VIRGO/SPM on-board the SoHO spacecraft. However, the frequency dependence of these variations is less clear, except for the frequency shifts $\Delta\nu_{n,\ell}$. But the changes in height, in linewidth and in velocity power show a maximum between 2.6 and 3.1 mHz, peaking near ∼2.8 mHz, which was already noted by Chaplin et al. (2000) for low degree modes and more clearly at higher angular degrees by Komm et al. (2000a). Only the energy supply rate seems not to show frequency dependence, as Komm et al. (2000b) have observed with GONG network observations.

5. Conclusion

The merging of IRIS, Mark-I and LOWL database in a consistent manner has provided 11 years of full disk observations. The reasonably good quality of the data, the annual duty cycles of around 60% and the duration covering a complete solar cycle

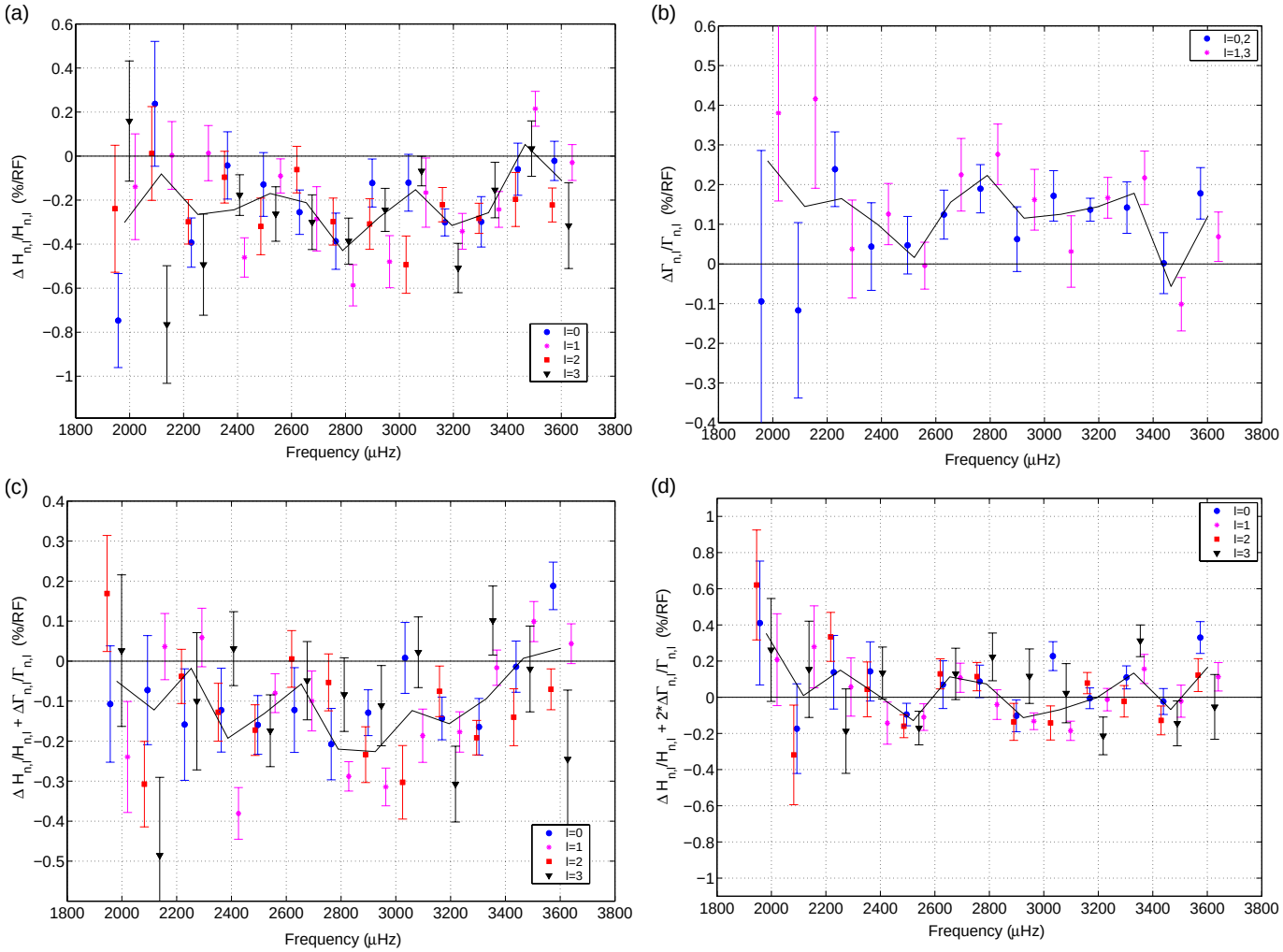

Fig. 6. Relative differences per unit of radio flux versus frequency for **a)** the height $H_{n,\ell}$, **b)** the linewidth $\Gamma_{n,\ell}$, **c)** the velocity power $<V^2_{n,\ell}>$ and **d)** the energy supply rate $\dot{E}_{n,\ell}$.

make this database particularly suitable to exploit the variation of the *p*-mode parameters.

Using timeseries of one year with an overlap of six months we have analyzed the *p*-mode parameter changes along the solar activity cycle. The mode frequency is the most sensitive parameter, increasing with higher activity. The observed frequency dependence is quite clear, being close to zero at 2 mHz and increasing progressively with frequency reaching a maximum of around 4 nHz/RF around 3.6 mHz, in good agreement with other works. We found a global change of about 0.28 μHz which seems slightly smaller compared to the previous cycle.

We found also clear evidences of the *p*-mode height and linewidth variations, uncovering a global change of about −26% and 11% respectively. The frequency dependence is less clear in both parameters; even a maximum near 2.8 mHz seems to be discerned. Concerning the linewidths, our results are in good agreement with what Houdek et al. (2001) have suggested: the decrease of the horizontal size of the solar granules from solar minimum to solar maximum observed by Muller (1988) at constant vertical size leads to an increase in the damping rates η between 2.4 and 3.0 mHz.

By means of these two parameters, we have calculated the velocity power of the modes as well as the energy supplied to them. In the case of the velocity power, we find a change of about −11% while the rate at which energy is supplied does not show an important variation clearly correlated with the solar cycle, implying that this remains constant with solar activity. However, we cannot confirm the increase in magnitude of the net forcing over a brief period in spring 1998 observed by Chaplin et al. (2003). A deeper analysis using shorter timeseries will be needed to confirm this observation.

Acknowledgements. Data from the IRIS network depends on the coordinated efforts of many people from several nations. The authors wish to thank those who have conceived the instrument: E. Fossat and G. Grec; those who have contributed to build and maintain all instruments on site: B. Gelly, J. F. Manigault, G. Rouget, J. Demarcq, G. Galou, A. Escobar, J. M. Robillot; those who have operated the observing sites: M. Baijumamov, S. Ehgamberdiev, S. Ilyasov, S. Khalikov, I. Khamitov, G. Menshikov, S. Raubaev, T. Hoeksema, Z. Benkhaldoun, M. Lazrek, S. Kadiri, H. Touma, M. Anguera, A. Jimenez, P. L. Palle, A. Pimienta, C. Regulo, T. Roca Cortes, L. Sanchez, F. X. Schmider; R. Luckhurst, those who have developed the analysis software: S. Ehgamberdiev, S. Khalikov, E. Fossat,

B. Gelly, M. Lazrek, P. L. Palle, L. Sanchez, E. Gavryuseva, V. Gavryusev; and those who have contributed to the success of the IRIS project in other critical ways: P. Delache, D. Gough, I. Roxburgh, F. Hill, T. Roca-Cortes, G. Zatsepin, T. Yuldashbaev, L. Woltjer, H. Van der Laan, D. Hofstadt, J. Kennewell, D. Cole, P. H. Scherrer, F. Sanchez, J. P. Veziant. The IRIS group is grateful to BiSON, IAC and HAO for sharing the Mark-I and LOWL data and acknowledges the LOWL observers Eric Yasukawa and Darryl Koon.
The Uzbek contribution has been supported by the Intas 97-31198 and SCOPES 7UZPJ065728.01/1 grants, and the cooperation between the IRIS group and LOWL has been supported by the CNRS/NSF cooperation.

References

Ahluwalia, H. S. 2002, in Amer. Phys. Soc., April Meet., 12 007
Anguera Gubau, M., Pallé, P. L., Pérez Hernández, F., et al. 1992, A&A, 255, 363
Appourchaux, T. 2001, Proc. of the SOHO 10/GONG 2000 Workshop: Helio- and asteroseismology at the dawn of the millennium, ESA SP-464, 71
Brookes, J. R., Isaak, G. R., & van der Raay, H. B. 1978, MNRAS, 185, 1
Chaplin, W. J., Elsworth, Y., Isaak, G. R., Miller, B. A., & New, R. 1999a, MNRAS, 308, 424
Chaplin, W. J., & Appourchaux, T. 1999b, MNRAS, 309, 761
Chaplin, W. J., Elsworth, Y., Isaak, G. R., et al. 2000, MNRAS, 313, 32
Chaplin, W. J., Elsworth, Y., Isaak, G. R., Marchenkov, K. I., Miller, B. A., & New, R. 2001, MNRAS, 322, 22
Chaplin, W. J., Elsworth, Y., Isaak, G. R., et al. 2003, ApJ, 582, L115
Christensen-Dalsgaard, J. 1989, MNRAS, 239, 977
Christensen-Dalsgaard, J., & Berthomieu, G. 1991, in Solar Interior and Atmosphere, ed. A. N. Cox, W. C. Livingston, & M. S. Matthews (Tucson: Univ. Arizona Press), 618
Duvall, T. L., Jefferies, S. M., Harvey, J. W., Osaki, Y., & Pomerantz, M. A. 1993, ApJ, 410, 829
Dziembowski, W. A., Goode, P. R., & Schou, J. 2001, ApJ, 553, 897
Fossat, E., Gelly, B., Grec, G., & Pomerantz, M. 1987, A&A, 177, L47
Gelly, B., Lazrek, M., Grec, G., et al. 2002, A&A, 394, 285
Goldreich, P., Murray, N., Willette, G., & Kumar, P. 1991, ApJ, 370, 752
Goldreich, P., Murray, N., & Kumar, P. 1994, ApJ, 424, 466
Houdek, G., Chaplin, W. J., Appourchaux, T., et al. 2001, MNRAS, 327, 483
Jiménez, A., Roca-Cortés, T., & Jiménez-Reyes, S. J. 2002, Sol. Phys., 209, 247
Jiménez-Reyes, S. J., Régulo, C., Pallé, P. L., & Roca Cortés, T. 1998, A&A, 329, 1119
Jiménez-Reyes, S. J., Corbard, T., Pallé, P. L., et al. 2001, A&A, 379, 622
Komm, R. W., Howe, R., & Hill, F. 2000a, ApJ, 531, 1094
Komm, R. W., Howe, R., & Hill, F. 2000b, ApJ, 543, 472
Komm, R. W., Howe, R., & Hill, F. 2002, ApJ, 572, 663
Kumar, P., Franklin, J., & Goldreich, P. 1988, ApJ, 328, 879
Libbrecht, K. G. & Woodard, M. F. 1990, Nature, 345, 779
Meunier, N. 1997, Ph.D. Thesis
Muller, R. 1988, Adv. Space Res., 8, 159
Nigam, R. & Kosovichev, A. G. 1998, ApJ, 505, L51
Pallé, P. L., Régulo, C., & Roca Cortés, T. 1990a, in Progress of Seismology of the Sun and Stars, ed. Y. Osaki, & H. Shibahashi (Springer-Verlag), 367, 189
Pallé, P. L., Régulo, C., & Roca Cortés, T. 1990b, in Progress of Seismology of the Sun and Stars, ed. Y. Osaki, & H. Shibahashi (Springer-Verlag), 367, 129
Press, W. H., Teukolsky, S. A., Vetterling, W. T., Flannery, B. P. 1992, in Numerical Recipes in Fortran, 2nd. edn. (Cambridge: Cambridge Univ. Press), 407
Salabert, D., Jiménez-Reyes, S. J., Fossat, E., et al. 2002a, Solspa 2001, Proc. of the Second Solar Cycle and Space Weather Euroconference, ESA SP-477, 253
Salabert, D., Fossat, E., Gelly, B., et al. 2002b, A&A, 390, 717
Salabert, D., Jiménez-Reyes, S., Fossat, E., & The IRIS Team 2002c, SF2A-2002: Semaine de l'Astrophysique Française, 531
Thiery, S., Boumier, P., Gabriel, A. H., et al. 2000, A&A, 355, 743
Tomczyk, S., Streander, K., Card, G., et al. 1995, Sol. Phys., 159, 1
Toutain, T., Appourchaux, T., Fröhlich, C., et al. 1998, ApJ, 506, L147
Woodard, M. F., & Noyes, R. W. 1985, Nature, 318, 449